

Dissolved gases in perennially ice-covered lakes of the McMurdo Dry Valleys, Antarctica

D.T. ANDERSEN¹, C.P. MCKAY² and R.A. WHARTON JR³

¹SETI Institute, NASA Ames Research Center, MS 245-3, Moffett Field, CA 94035, USA

²Space Sciences Division, NASA Ames Research Center, MS 245-3, Moffett Field, CA 94035, USA

³Desert Research Institute, PO Box 60220, Reno, NV 89506, USA

Abstract: Measurements of dissolved N₂, O₂, Ar, CO₂, and CH₄ were made in perennially ice-covered Lake Hoare. Results confirm previous reports that O₂ concentrations in the upper water column exceed atmospheric equilibrium and that N₂ and Ar are supersaturated throughout the water column. The mean supersaturation of N₂ was found to be 2.0 (±0.37) and Ar was 3.8 (±1.1). The ratios of N₂/Ar (20.3 ±3.8), and O₂/Ar (22.5 ±4.0) at the ice-water interface are consistent with those previously measured, suggesting that bubble formation is the main process for removing gas from the lake. However, the saturations of N₂ and Ar greatly exceed those previously predicted for degassing by bubble formation only at the ice-water interface. The data support the hypothesis that removal of gas by bubbles occurs in the water column to a depth of 11 m in Lake Hoare. CO₂ concentration increases from near zero at the ice-water interface to 80–100 times saturation at and below the chemocline at *c.* 28 m. There is considerable variability in the gas concentrations throughout the water column; samples separated in depth by one metre may vary by more than 50% in gas content. It is likely that this phenomenon results from the lack of turbulent mixing in the water column. Methane (*c.* 2 µg l⁻¹) was detected below the chemocline and immediately above the sediment/water interface at a depth of 30 m. Samples from lakes Vanda, Joyce, and Miers, also show supersaturations of O₂, N₂, and Ar at levels similar to levels found in Lake Hoare.

Received 11 June 1997, accepted 23 February 1998

Key words: Antarctica, dissolved gases, perennially ice-covered lakes, supersaturation

Introduction

The McMurdo Dry Valleys of Antarctica contain perennially ice-covered lakes that are interesting in that they neither freeze solid in the winter nor thaw completely during the summer (Chinn 1993). In this paper data are presented on dissolved gases within four of these lakes; Hoare, Joyce, Vanda and Miers. It has previously been recognized that the O₂ and N₂ concentrations in the water column exceed atmospheric equilibrium (Vincent 1988, Simmons *et al.* 1993, Wharton *et al.* 1993). There are both biological and non-biological sources of gas within the lakes. However, the contribution of each these sources to the overall gas budgets are not well understood.

Most of the data are derived from the analysis of samples obtained at Lake Hoare (77°38'S, 162°53'E), a perennially ice-covered, oligotrophic, amictic lake located in the eastern end of Taylor Valley at an elevation of 58 m. It is 4.1 km long, 1.0 km wide and has a maximum depth of 34 m with a mean depth of 14.2 m. The lake is dammed at its eastern end by the Canada Glacier, an alpine glacier flowing into the valley from the Asgard Mountains. Lake Hoare receives water and sediments from glacial melt and from Lake Chad during the summer (Wharton *et al.* 1993).

Wharton *et al.* (1987) and Craig *et al.* (1992) discussed quantitative models of both O₂ and N₂ in Lake Hoare. In their

models of gas flow into and out of the lake they considered both biological and non-biological sources and sinks. Gases enter the lake as air dissolved in water and are concentrated in the water column as water freezes onto the bottom of the ice-cover. The presence of the ice-cover prevents the dissolved gases in the water from mixing freely with the atmosphere. Water leaves the lake by sublimation from the top of the ice cover. Bubbles are present in the ice cover and are a major sink for gases from the lake. In addition to loss through bubbles in the ice, there may be some loss of gases through the peripheral moat that forms on the shore each summer (Parker *et al.* 1981, Wharton *et al.* 1987). The noble gases have no known biological sources or sinks and one could expect a build-up of these gases in the water column. Biological processes should have the most pronounced effect on O₂, CO₂ and CH₄ concentration due to photosynthesis and respiration, as well as anaerobic conditions that are found in Lake Hoare below *c.* 28 m. Biological sources and sinks for N₂ are small compared to the dissolved input (Allnut *et al.* 1981, Vincent *et al.* 1981, Wharton *et al.* 1987, Voytek *et al.* 1995). Net production of O₂, due to removal of organic material via burial in the sediments, will affect the O₂ concentrations to a much larger extent than they will affect N₂, thus altering the N₂:O₂ ratio (Wharton *et al.* 1987). Therefore, this ratio can be a useful "signature" of the relative strengths of biological and

non-biological gas production. In Lake Hoare, this ratio was 1.20 at the ice/water interface and 1.05 at 12 m; considerably different from the ratio in equilibrium with air (*c.* 1.8). Based upon the above results, Wharton *et al.* (1987) suggested that about half of the net O₂ production in Lake Hoare is the result of biological processes. Wharton *et al.* (1986) also pointed out that biological processes can cycle O₂ in the water column without contributing to the net source of O₂.

As reported by Craig & Hayward (1987) and Craig *et al.* (1992), the exsolution of gas to form bubbles fractionates N₂, O₂, and Ar. This effect is similar for O₂ and Ar, which have similar solubility coefficients. However, there is a large fractionation of N₂ when compared to either O₂ or Ar because the solubility coefficients differ by a factor greater than 2. Since bubble formation constitutes a major loss of gas from the lake, the different solubility coefficients of N₂ and O₂ make it difficult to determine the biological source of O₂ production from N₂ and O₂ measurements alone. Craig *et al.* (1992) measured N₂, Ar, and O₂ content of bubbles in ice samples from Lake Hoare. By comparing the N₂/Ar ratio to the O₂/Ar ratio, Craig *et al.* (1992) found that the extent of biological processes may be lower than estimated by Wharton *et al.* (1987). They concluded that only 11% of the O₂ is of biological origin. To further the work described above, additional samples were collected at Lake Hoare of water column gases from the ice water interface to a depth of 30 m.

Methods

N₂, O₂, Ar, CO₂, and CH₄ concentrations were measured in the water column of Lake Hoare at 1 m intervals from the ice-water interface to the lake bottom. Additional samples were obtained at lakes Vanda, Miers and Joyce. Sample depths for these lakes are shown in Table I. Samples were obtained during the 1994 summer (December and January). The samples were collected using 150 ml glass serum bottles (Wheaton Scientific) fitted with a flange style, red rubber stopper and sealed with an aluminium crimp. Prior to shipment to Antarctica, each bottle was evacuated using a high vacuum mechanical pump and mercury diffusion pump to approximately 10⁻⁷ torr. Upon arrival at McMurdo and prior to sampling, each bottle received a 2.5 ml (@ STP) injection of Kr (99.999%, Matheson Gas Products) as an internal standard and to correct for the loss of gas from the sampling needle during the analysis of the pressurized head space. During analysis the needle is moved from the higher pressure inside the head space to ambient before injection into the gas chromatograph. This loss of gas was corrected using the known Kr amounts by normalizing the results with a linear function of pressure.

Water samples were collected at Lake Hoare near the centre of the lake using a mechanical sampling device lowered through a hole *c.* 5 cm in diameter. With this device, a single bottle could be lowered to the prescribed depth and by pulling on a second cable, a needle (22 gauge) was inserted into the

Table I. Dissolved gas data for lakes Joyce, Vanda and Miers.

Lake	Depth m	S _{O₂} ^a	S _{N₂} ^a	S _{Ar} ^a	S _{CO₂} ^a	N ₂ /Ar	O ₂ /Ar
Joyce	15.0	3.6	2.2	3.3	0.19	24.6	22.6
	25.0	1.0	3.5	5.7	28.2	22.3	3.6
	30.0	0.6	3.0	5.8	31.3	19.2	2.2
Vanda	40.0	2.5	2.7	2.4	1.1	41.5	21.3
	58.0	2.2	3.1	2.4	7.7	48.0	19.3
Miers	5.0	2.5	2.3	2.5	0.22	34.0	20.9
	10.0	2.4	2.3	[3.2] ^b	1.9	[26.4]	[15.6]

^a S_x of gas "x". Saturation is defined as the volume concentration of gas divided by the value that would be found in water in equilibrium with the atmosphere at a total pressure of moist air of 1 atm (Weiss 1970).

^b Numbers in [] indicate data corrected by an apparent drop of one decimal place in S_{Ar}.

bottle through the stopper. Releasing the cable allowed a counterweight to retract the needle from the bottle. Several trial runs allowed us to estimate the time required for filling the serum bottle with water, forming a headspace by compressing the internal standard to the local hydrostatic pressure. Upon retrieval the bottles were dried and a small amount of Apiezon type N grease was applied to the stopper as an additional seal. They were placed into an insulated container to prevent freezing.

Upon return to the Crary Science and Engineering Center, the samples were analysed for N₂, O₂, Ar, Kr, CO₂, and CH₄ by injecting 10 or 250 µl aliquots of head space gas into a Hewlett Packard 5890-II gas chromatograph (GC) fitted with a J&W Scientific molesieve column (#115-3632) and a thermal conductivity detector. The initial column temperature was maintained at -50°C for 1 min to facilitate the separation of Ar and O₂ and then raised steadily (20°C min⁻¹) to 220°C to remove CO₂, water vapour and any other contaminants. The injector and detector temperatures were set at 250°C and 300°C, respectively.

The instrument was calibrated using injections of laboratory air as the source for a nominal air standard. Three commercially prepared gas standards purchased from Scott Speciality Gases were also used for calibration and for peak identifications of N₂, O₂, Ar, Kr, CO₂, and CH₄. The three calibration standards were composed of the following:

- 1) Noble gas standard – Ne at 2.04%, Ar at 2.00% and Kr at 2.05%, the remainder being air;
- 2) CO/CO₂ standard – CO at 2.00%, CO₂ at 2.00%, O₂ at 18.00%, the remainder being N₂;
- 3) CH₄ standard – CH₄ at 5.005% with the remainder being N₂.

Standards were analysed after every five samples to eliminate any error due to instrument drift.

Although the serum stoppers provided a good seal, a very small amount of gas vented through the needle hole in some of the bottles. Leakage occurred particularly in those bottles

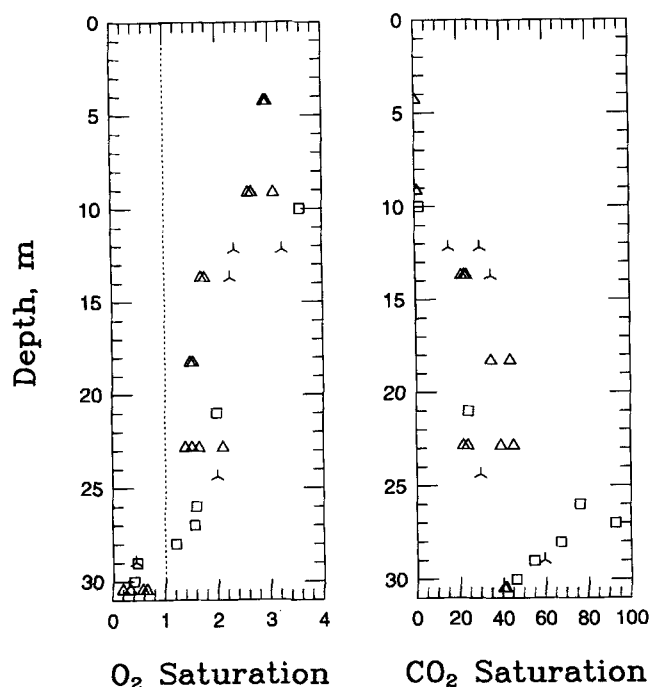


Fig. 1. Saturation values for O_2 and CO_2 versus depth in Lake Hoare. Samples from a given date are labelled with the same symbol: 18 Dec. 1994 – triangles; 12, Jan 1995 – squares; 4 Jan 1995 – tripods. The uncertainty in depth is less than 0.5 m. The dotted line refers to the value expected for water in equilibrium with the atmosphere at $0^\circ C$. Standard errors for O_2 and CO_2 replicates are 5% and 13% respectively (see text).

returned from depths greater than 20 m, as a result of high internal pressure. This loss was not significant as could be determined from the Kr internal control. In addition, because the gas ratios in air are different from the ratios of gas exsolved from water, air leaks during shipment could be detected by the GC, as well as by anomalous head space volumes. Such samples were discarded. Confirmation that the sample bottles held vacuum for several months before use was obtained by noting the volume of the headspace after the bottles filled with water. The samples were analysed within two weeks of their collection.

Error has been estimated in the following manner. At five depths replicate samples were obtained and for each such depth and for each gas the standard deviation of the replicates was determined. These were averaged for each gas. The results are O_2 :5% ($S_o > 1$), N_2 :10.2%, Ar:12.6%, CO_2 :13%, N_2/Ar :11%, O_2/Ar :12% ($S_o > 1$). The largest replicate error for N_2 or Ar is $\pm 21\%$ for Ar at 9 m. Note that for samples from Lake Hoare to which 2.5 ml of Kr @ STP was added, the measured value of Kr amount was 2.5 ml $\pm 9.6\%$. Therefore an overall 10% error has been assigned to our results. In this paper the term saturation, S_x , is used for each gas species, x, to be defined as the volume concentration of gas divided by the value expected in water in equilibrium with the atmosphere at a total pressure of moist air of 1 atm.

Results

The saturation of O_2 , CO_2 , N_2 , and Ar are plotted as a function of depth (Figs 1 & 2). At unity saturation, the concentration of N_2 , O_2 , and Ar are 18.2, 10.1, 0.49 ml (STP)/kg, respectively (Benson & Krause 1976, Craig *et al.* 1992). All three of these gases are supersaturated just beneath the ice-cover ($S_N = c. 2.0$, $S_o = c. 3.5$, $S_{Ar} = c. 3.5$). The saturation of O_2 decreases, roughly linearly, toward the bottom of the lake and falls to negligible values near the bottom. The mean saturation for N_2 is 2.0 with a standard deviation of ± 0.37 and for Ar, 3.8 with a standard deviation of ± 1.1 . There is considerable variability in the gas concentration with depth and time. This variability has been observed in previous measurements of dissolved O_2 (Wharton *et al.* 1986). The N_2 and Ar data do show a slight trend with depth. Statistical analysis indicates that both sets of samples have a correlation coefficient of 0.7, which for 33 samples gives a probability that the linear dependence is valid of more than 99.9% (Bevington 1969). The slope for Ar corresponds to a change of 60% in concentration from the surface to 30 m and 41% for N_2 . It might be speculated that the gradient in the concentrations of N_2 and Ar in the deep water is a reflection of the increased meltwater inflow and the thinning of the ice cover over the past decade (Chinn 1993, Wharton *et al.* 1993). Because these differences are comparable to our measured errors and because systematic errors due to pressure in the sampling vessels may affect depth dependence we do not consider further this slight increase in Ar and N_2 gas with depth.

Figure 1 also shows the measured saturation of CO_2 . The partial pressure of CO_2 depends on the carbonate equilibrium of the lake water and does not simply follow Henry's Law as it would in pure water. Since the head space volume is small compared to the water sample, and because the solubility coefficient of CO_2 is relatively high, we estimate that c. 3% of the CO_2 is present as head space gas. This amount represents a negligible change in the CO_2 carbonate system, and thus the data provide a direct measurement of the CO_2 fugacity in the water column. The results are reported in terms of the equilibrium solubility in pure water, i.e. assuming Henry's law; thus a saturation of unity corresponds to the ambient CO_2 partial pressure (c. 350 μatm). The direct measurement of CO_2 complements chemically based analytical methods (Cole *et al.* 1994). In this context it should be noted that measurements taken with a HydroLab DataSonde 3 (HydroLab Inc., Austin TX) indicate that the pH is about 8.2–8.6 in the upper 10 m and then drops sharply to about 7.3 at 15 m and remains constant below that depth, consistent with the CO_2 results. CO_2 increases with depth to the top of the chemocline reaching maximum values of 100 times saturation before decreasing by a factor of 2 through the chemocline to the bottom.

Methane was detected in two samples taken from within the anaerobic zone giving concentrations of 1.0 and 2.5 $\mu g l^{-1}$. These data indicate the presence of methane-producing bacteria

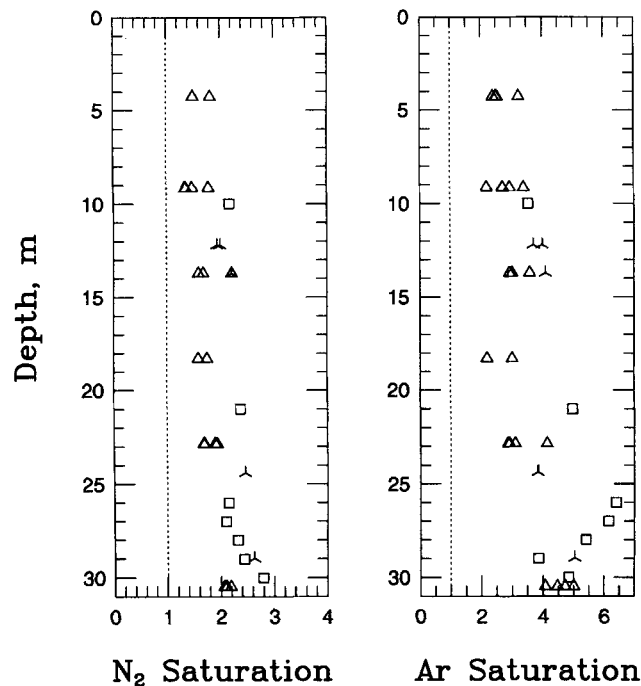


Fig. 2. Saturation values for N_2 and Ar versus depth for all locations sampled in Lake Hoare. The dotted line refers to the value expected for water in equilibrium with the atmosphere at 0°C . Symbols as in Fig. 1. Standard errors for N_2 and Ar replicates are 10% and 13% respectively (see text).

in the anaerobic zone within Lake Hoare. The lack of CH_4 in the water immediately above the chemocline suggests the presence of CH_4 oxidizing bacteria (Galchenko 1994, Franzmann *et al.* 1991). Observations made by divers indicate that a visible bacterial haze occurs at the oxic/anoxic interface about 2 m above the lake bottom. Since some loss of CH_4 due to microbial oxidation may have occurred during transport and storage, these results represent a lower limit.

Table I presents the results from a limited number of samples obtained from lakes Joyce, Miers, and Vanda. All samples from these lakes show supersaturation of N_2 and Ar at levels similar to those found in Lake Hoare. The N_2/Ar ratios in Miers and Vanda are much larger than in Hoare, which may be a result of differences in the ice cover and basin morphology.

Discussion

One striking feature of the results is the large variability in the gas concentration seen in Lake Hoare. Samples from the same location vertically separated by 1 m can have gas concentrations that differ by 50%; the N_2/Ar ratio (Fig. 3) varies as well but by a smaller factor. This variability does not correlate with sampling or analytical procedures and is probably a natural occurrence, likely a result of the lack of turbulent mixing in the water column.

The variability in our data is comparable to the variability

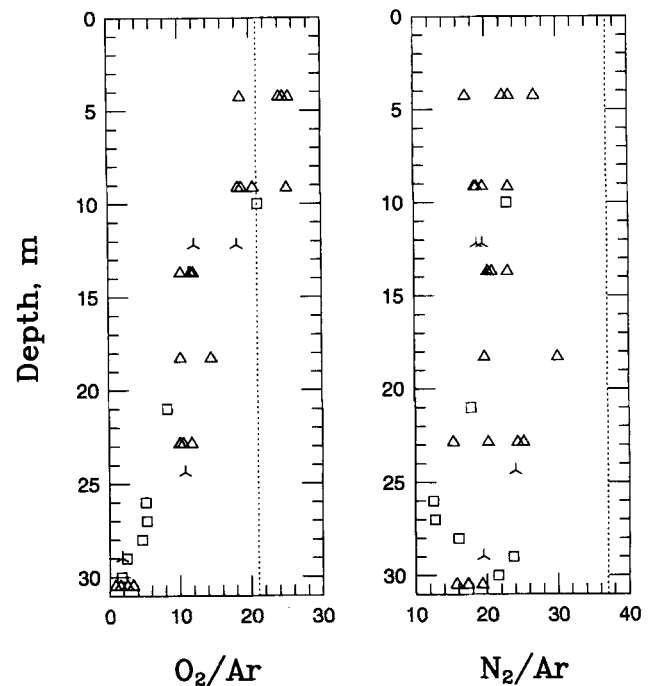


Fig. 3. Ratios of N_2 and O_2 to Ar versus depth for Lake Hoare. The dotted line refers to the value expected for water in equilibrium with the atmosphere. Symbols as in Fig. 1.

in the O_2 data reported by Wharton *et al.* (1986). Their data show variations that occur day to day, at equal depths and between depths that are comparable to the variations seen in Fig. 1. This is an additional indication that the variability is a naturally occurring phenomenon and not simply a result of sampling error. As discussed below, this variability probably results from low eddy mixing in Lake Hoare.

Figure 3 shows the N_2/Ar and O_2/Ar ratios in these data. The N_2/Ar ratio shows no clear trend with depth, which would be expected because these gases have no significant sources or sinks in the water column. The average value of N_2/Ar is 20.3 ± 3.8 . This can be compared (Fig. 4) with the N_2/Ar measured by Craig *et al.* (1992) in bubbles in the ice cover.

Craig *et al.* (1992) developed a model for the freezing process. They considered a unit mass of water freezing at the bottom of the ice cover. In developing their model they made the following assumptions:

- 1) bubble formation occurs as soon as the gas pressure exceeds local hydrostatic pressure;
- 2) the unit mass of water remains in complete equilibrium with the bubble throughout the freezing process;
- 3) the unit mass of water and ice remains materially isolated and after some degree of freezing the residual water is removed from the ice-water interface carrying with it some remnant of the dissolved gases;
- 4) the bubble in the ice cover is then closed and retains the

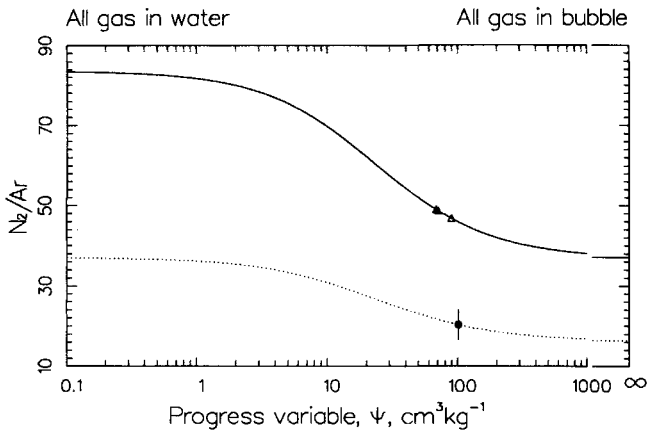


Fig. 4. Ratios of N₂ to Ar as a function of ψ predicted by the Craig *et al.* (1992) freezing model for gas in a bubble (solid line) and in the residual liquid (dotted line). The parameter ψ indicates the extent of freezing; $\psi = 0$ is the start of the freezing process; $\psi = \infty$ is the end of the freezing process. The data of Craig *et al.* for the ice cover bubbles are shown as triangles. The mean N₂/Ar ratio (20.3±3.8) is shown by the solid circle with error bars.

signature of this freezing process.

Based on this scenario, Craig *et al.* (1992) developed a formalism that relates the N₂/Ar and O₂/Ar ratios to a “progress variable”, ψ (measured in ml gas at local pressure per kg of residual liquid) which is defined as the ratio of the bubble volume formed within the ice (at ambient pressure) to the mass of the water remaining at any point in the freezing process within an isolated system.

Consider a unit mass of meltwater. Mass balance for each gas requires that the gas dissolved in the incoming meltstream equals the gas in the bubble plus that in the residual liquid. This can be expressed as

$$X_i^{air} P_a b_i = X_i P_g V_b + X_i P_g b_i M_l \quad (1)$$

Where X_i^{air} is the mixing ratio of gas “i” in the atmosphere, P_a is the atmospheric pressure, b_i is the solubility coefficient for gas “i”, X_i is the mixing ratio of gas “i” in the bubble, P_g is the local hydrostatic pressure and the pressure in the bubble, V_b is the volume of the bubble and M_l is the mass of the remaining liquid. Equation 1 together with

$$\sum_i X_i = 1 \quad (2)$$

and the definition

$$\psi = V_b / M_l \quad (3)$$

contributes the set of equations used in the Craig *et al.* (1992) model.

The Craig *et al.* (1992) freezing model is shown schematically in Fig. 5. It is important to note that $\psi = 0$ represents the start of bubble formation, not the onset of freezing. When $\psi = 0$, all gas is present as dissolved gas within the residual liquid. Accordingly, the total pressure of dissolved gas is equal to the local hydrostatic pressure. Any further freezing raises the total gas pressure above the local hydrostatic pressure and a bubble forms. Freezing without bubble formation occurs when the inflowing liquid has a total gas pressure that is less than the local hydrostatic pressure where freezing occurs. Craig *et al.* (1992) consider a 5 m thick ice cover implying that the hydrostatic pressure at the ice-water interface is 1.45 atms. As ψ approaches infinity the water is completely frozen and the gas exists entirely in the form of a bubble in the ice. The intermediate stage shown in Fig. 5 corresponds to $\psi = 71$, which is the typical value found by Craig *et al.* (1992). At this value of ψ , for the freezing of meltwater at 0°C, approximately 80% of the water exists in the frozen state ($M_l = 0.2$) and 75% (1–1.27x0.2) of the N₂, 58% of the O₂, and 56% of the Ar have been forced into the bubble.

Numerical results for the Craig *et al.* model are tabulated in Table II for ψ values ranging from 0 to infinity. The ratio of gases in the liquid phase (subscript l) and gas in equilibrium with this liquid (subscript g), as well as the saturations of the gases are also listed in Table II. The final column in Table II, M_l , shows the mass of remaining liquid divided by the initial mass of liquid. All numbers in Table II, except ψ , are quantities without dimension. The total gas pressure of the incoming meltwater (the first row in Table II) is less than the local hydrostatic pressure, therefore bubbles would not be expected to form. Freezing therefore proceeds without bubble formation and the concentration of all gases in the residual water increases uniformly; the gas ratios remain unchanged. Bubble formation begins when the total pressure of dissolved gases equals 1.45 atms. This corresponds to $\psi = 0$ (the second row in Table II). It should be noted that the total pressure of

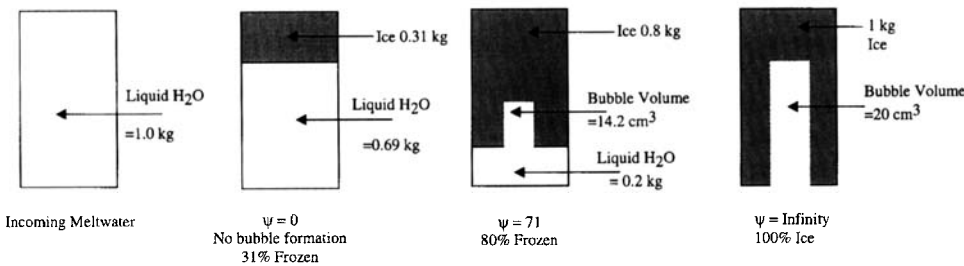


Fig. 5. The Craig *et al.* (1992) freezing model is shown schematically beginning with a parcel of incoming meltwater at $\psi = 0$ and progressing to $\psi = \infty$ with the parcel of water completely frozen and all of the dissolved gas having been exsolved into a bubble.

Table II. Numerical results for the Craig *et al.* (1992) model.

ψ	N_2/Ar_{gas}	O_2/Ar_{gas}	N_2/Ar_{liq}	O_2/Ar_{liq}	S_{Ar}	S_N	S_O	M_i
Melt ^a	83.60	22.43	37.00	20.53	1	1	1	1
0	83.60	22.43	37.00	20.53	1.45	1.45	1.45	0.69
1	81.72	22.39	36.17	20.49	1.48	1.44	1.47	0.66
10	69.79	22.11	30.89	20.24	1.67	1.40	1.65	0.50
71	48.68	21.31	21.54	19.50	2.19	1.27	2.08	0.20
100	45.94	21.15	20.33	19.36	2.28	1.25	2.15	0.15
1000	38.08	20.62	16.85	18.87	2.60	1.18	2.39	0.02
10000	37.11	20.54	16.42	18.80	2.65	1.18	2.42	0.002
∞	37.00	20.53	16.38	18.79	2.65	1.17	2.43	0.00

^aMelt refers to the incoming meltwater at $S=1$.

dissolved gases is always equal to 1.45 atms for all values of $\psi > 0$.

In an ideal closed system, when $\psi = 0$, the gases in the water have N_2/Ar and O_2/Ar ratios still determined by equilibrium with the atmosphere (37 and 21 respectively). The gas within a bubble in equilibrium with this water would resemble atmospheric composition (84 for N_2/Ar and 22 for O_2/Ar). As ψ becomes larger than zero and continued freezing takes place, more dissolved gas in the water is forced into a bubble in the ice. At any point in the freezing process, the partial pressure of each gas in a bubble is in equilibrium with the amount of that same gas dissolved in the residual water. Thus, the initial concentration of each gas is partitioned between the bubble and the dissolved gas remaining in the water and is dependent on its solubility coefficient. As a result, for any finite amount of freezing ($\psi > 0$) the gas in the bubble does not have the same composition as air but contains a mixture that reflects the inventory and the relative solubility of the gases in water. Importantly, the mixture is depleted in N_2 with respect to air. When the limit of ψ becomes infinite, the water is completely frozen and all the gas that was initially dissolved in the water has exsolved into the bubble. In this case the gas within the bubble must have the same ratios as the gas initially dissolved in the water before any freezing began (37 for N_2/Ar and 21 for O_2/Ar). The ratios in the water at $\psi = 0$ are equal to the ratios in the bubble at $\psi = \infty$. For values of ψ between zero and infinity the ratios will have intermediate values.

In Fig. 4 we show the N_2/Ar ratio, as a function of ψ , expected in a bubble (solid line) in the ice and the residual water (dotted line) in equilibrium with that bubble. The values of Craig *et al.* (1992) for the bubbles in the ice cover are shown as triangles. They suggest a value of ψ of 71. Shown in Fig. 4 is our average value of N_2/Ar for the residual water of 20.3. Our results are consistent with those of Craig *et al.* (1992) suggesting that bubble formation plays a key role in determining the N_2/Ar ratio in the lake.

As described above, the model of Craig *et al.* (1992) can also be used to predict the expected supersaturation of gas in the water column. As freezing proceeds, the saturation of N_2 decreases while those of O_2 and Ar increase. Results have

been plotted in terms of N_2 versus Ar saturation, (Fig. 6). The data range from 1 to 3 for S_N and from 1 to 7 for S_{Ar} . Inflowing meltwater in equilibrium with the atmosphere would have S_N and S_{Ar} values of unity. The dashed line shows how the gas concentration would increase if all gases were retained in the water as freezing progressed. N_2 and Ar concentrations would increase linearly and the N_2/Ar ratio would remain constant, unaltered by biological activity. O_2 concentrations would be subject to alteration by biological processes in the lake. In this case arbitrarily large supersaturations would be reached in the residual liquid. The solid line in Fig. 6 shows how the dissolved gas concentration would change following the Craig *et al.* model (1992). It should be noted that the point $\psi = 0$ occurs at $S_N = S_{Ar} = 1.45$. This is because the gases must be concentrated to this level before bubbles can form at a depth of 5 m, the ice thickness assumed by Craig *et al.* (1992). Thus, there will be a period of ice formation before bubbles begin to form. The value $\psi = 0$ represents the start of bubble formation; ψ approaching infinity represents complete freezing. The point, $\psi = 71$, suggested by Craig *et al.* (1992) as the point at which a bubble becomes isolated from the liquid by occlusion in the ice, is also indicated. The ultimate saturations reached by following the Craig *et al.* model are 1.17 for S_N and 2.43 for S_{Ar} (see Table II). Figure 7 shows the N_2/Ar ratios as a function of the Ar saturation. The solid line shows the expected results from the model by Craig *et al.* (1992). Note that our measurements and analyses pertain only to the central part of the lake. It is expected that there is some gas loss through the summer moat (Wharton *et al.* 1986), which may be as high as 25% of the gas budget (Craig

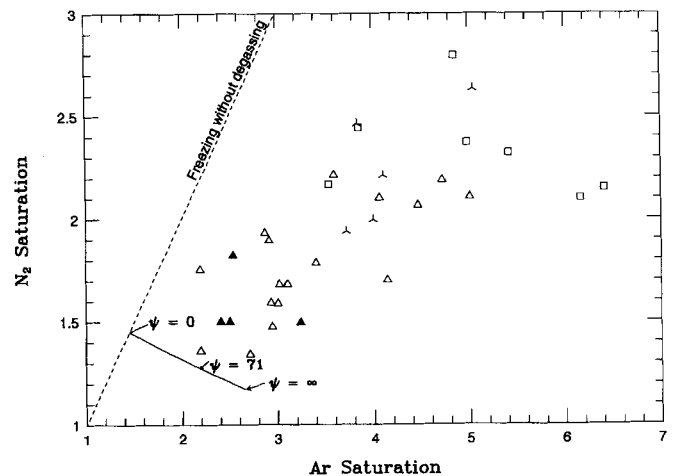


Fig. 6. Saturation of N_2 versus Ar. The dashed line indicates the expected values for water that freezes while retaining all of the dissolved gases in the residual liquid. The solid line is the freezing model of Craig *et al.* (1992). The value of $\psi = 71$ was suggested by Craig *et al.* based on gas ratios in ice-cover bubbles from Lake Hoare. Our data are represented as open squares and fall primarily between the two lines. Symbols as in Fig. 1 and the four points at the ice-water interface have been filled in.

et al. 1992). If the loss from the moat is this large, then one would expect a measurable gradient in the dissolved gas concentration, as well as fractionation by solubility and isotope in a transect from the centre of the lake to the shore.

Clearly, the concentrations of N_2 and Ar we have measured in the water column of Lake Hoare do not correspond strictly to the Craig *et al.* (1992) model nor do they follow the line expected for freezing without bubble formation. Indeed, the data seem to be bounded by these lines. However, the agreement of our N_2/Ar ratio at the ice-water interface with the predictions of the Craig *et al.* (1992) model (Fig. 4) imply that the basic gas concentration process proposed in the model – gas exsolution upon freezing – and the concomitant fractionation of N_2 , Ar and O_2 is valid. Other assumptions made by Craig *et al.* (1992) may be invalid, in particular: assuming bubble formation occurs immediately when gas pressure exceeds hydrostatic pressure and considering the bubble and residual liquid acts as a closed system. Gas concentrations in the water column may reach values much higher than predicted by the Craig *et al.* model because the onset of bubble formation does not occur until the pressure of dissolved gases greatly exceeds the local hydrostatic pressure, or because not all of the gas in the freezing layer can diffuse to the bubble sites as freezing progresses. It is important to note that due to differing solubilities, N_2 is systematically depleted with respect to Ar in the water column, as indicated by the N_2/Ar ratio in Figs 3 & 7. All ratios are below the value ($N_2/Ar = 37$) expected for freezing without bubble formation. This indicates that the main gas-removal mechanism is associated with bubble formation. The low solubility of N_2 compared to Ar, ensures that N_2 is preferentially degassed into a bubble when that bubble is in contact with the water. Observations do not imply that bubble formation occurs only at the ice-water interface as assumed in the Craig *et al.* model.

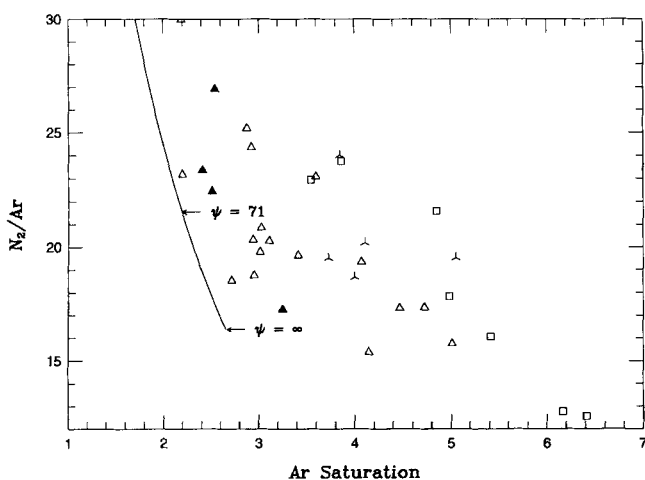


Fig. 7. Ratio of N_2 to Ar versus Ar saturation for Lake Hoare. The solid line are the results predicted by the freezing model of Craig *et al.* (1992). The parameter ψ is as defined in Fig. 4. Symbols as in Fig. 1, and the four points at the ice-water interface have been filled in.

As shown in Fig. 7, the data do not conform to the predictions of the Craig *et al.* model. Bubbles may form at depth and rise while removing and fractionating supersaturated gases from the water column.

It is possible that freezing results in highly saturated “parcels” of water that exhibit gas pressures in excess of hydrostatic pressure. During the freezing process bubble formation depletes some of the dissolved gases but the water is not in equilibrium with the ice-cover bubbles and is not limited to the Craig *et al.* values. Instead supersaturations may reach levels of 5 or more. Both experimental and theoretical studies indicate that the pressure of dissolved gas must exceed the local hydrostatic pressure before bubbles form (Carte 1961, Bari & Hallett 1974, Lipp *et al.* 1987). The supersaturation of gas required before bubbles form depends on the rate of freezing but supersaturations larger than 10 are possible (Bari & Hallett 1974).

Our data can be used to address the stability of bubbles in the water column below the ice-water interface. Wharton *et al.* (1986) were the first to report that lift-off mats – bubble-laden microbial mats rising to the ice-water interface – were related to the supersaturation of non-oxygen gases in the water column. By noting that the lift-off mat occurred only to a depth of *c.* 11 m, they predicted that the N_2 saturation at that depth must be 2. This value is essentially identical to the mean N_2 saturation levels we obtain (2.0 ± 0.37). Figure 8 shows the ratio of total pressure of dissolved gas divided by the local hydrostatic pressure. The total gas pressure, P_{gas} , is given by (neglecting the small vapour pressure of water and CO_2):

$$P_{gas} \text{ (atms)} = 0.78 S_N + 0.21 S_O + 0.01 S_{Ar} \quad (4)$$

In Fig. 8 the mean value for S_N and S_{Ar} have been used in

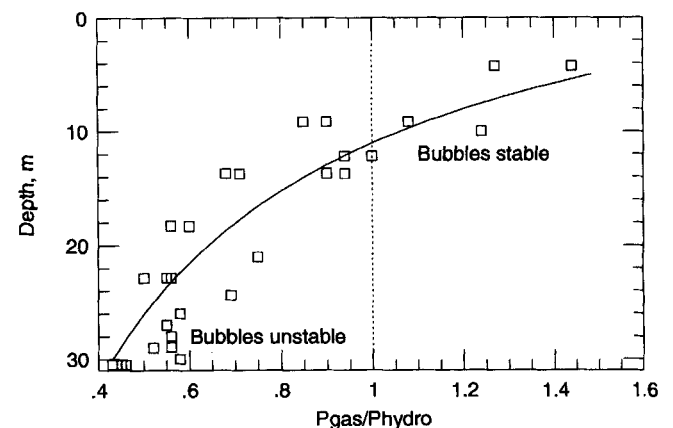


Fig. 8. Total pressure of dissolved gas (P_{gas}) for the average values of the measurements for Lake Hoare (see text) divided by the local hydrostatic pressure (P_{hydro}), shown by solid line. Individual samples are shown by squares. When this ratio exceeds unity, bubbles in the water column grow, limited only by diffusion of gas to the bubble site. Bubbles are stable above 11 m.

Equation 4. For S_0 a least squares fit to a straight line has been used. Thus, the curve represents the average conditions in the water column. When P_{gas} exceeds the local hydrostatic pressure bubbles would be stable. Any bubble will grow with time, its growth being limited by the diffusion rate of gas through the water column to the bubble. Bubbles will dissolve when P_{gas} is less than the local hydrostatic pressure. As can be seen in Fig. 8, bubble stability occurs for depths less than 11 m. The nucleation of bubbles within the stability region may be governed by the presence of micro-organisms, and the bubbles, in turn, may affect their buoyancy regulation in the water column.

It is possible to use the observed gradient in the oxygen concentration to determine the downward flux of O_2 in the water column. The downward flux results from the biological consumption of O_2 in the lake. This flux represents a cycling of O_2 in the lake and does not provide information about a net source or sink. O_2 is returned to the water column by the upward flux of CO_2 , indicated by the CO_2 gradient in Fig. 1. The flux of oxygen, FO_2 , is given by

$$FO_2 = -(D+K) dO_2/dz \quad (5)$$

where D is the molecular diffusion coefficient and K is the turbulent (eddy), mixing coefficient. The value for D is expected to be about $2 \times 10^{-5} \text{ cm}^2 \text{ s}^{-1}$; the value for K is unknown due to the uncertain level of eddy mixing.

The O_2 gradient can be compared with the net upward flux of CO_2 in the lake using the data shown in Fig. 1. As the transport coefficient is unknown, only the gradients can be compared. The O_2 gradient is equivalent to $-1.0 \times 10^{-3} \pm 0.3 \text{ ml gas at STP/l water per metre}$ and the CO_2 gradient is equal to $1.3 \times 10^{-3} \pm 0.3 \text{ ml gas at STP/l water per metre}$. This suggests that within the uncertainties, the fluxes are equal and opposite. The net biological production (or loss) of O_2 in the lake represents the difference between these fluxes. A more precise treatment of the coupled carbon and oxygen budget of the lake is required to determine the net flux.

In addition, the biological cycling of O_2 in the lake can be compared to the inflow of O_2 in the dissolved meltwater. The meltwater brings in about 30 cm yr^{-1} of water at $S_0=1$ (Wharton *et al.* 1986). Using only the molecular diffusion coefficient D in Equation 5, the biological flux of O_2 downward through the lake is equivalent to the O_2 flux carried by 0.6 cm yr^{-1} of water with $S_0=1$, which is 50 times smaller than the meltwater inflow. However, there is certainly some eddy transport of O_2 . Ellis *et al.* (1991) studied thermal diffusion in an ice-covered lake and noted that the thermal diffusion coefficients increased from a value close to molecular diffusion at the ice boundary to 10 times larger a few metres below the ice-water interface. Gu & Stefan (1990) used an eddy diffusion coefficient under an ice cover that varies from 1 to 10 times the molecular diffusion value. Unlike many of the other McMurdo Dry Valley lakes, Lake Hoare is isothermal. Accordingly, the Richardson Number (Ri) is zero and eddy diffusion occurs in neutral conditions. In this case eddy

transport is proportional to the shear stress usually resulting from wind. In Lake Hoare, wind is not a major factor but shear could be induced in the lake from the inflowing meltwater or perhaps by wind action on the summer moat. A direct measurement for a value for K was not possible, but it is likely to be 10 times D . In this case the flux of O_2 resulting from biological processes in the lake is comparable to, but still smaller than, the net amount of O_2 carried into the lake by the meltstream. Thus O_2 may be cycled rapidly by biological processes, even if there is negligible net biological production of O_2 . For an eddy coefficient of $2 \times 10^{-4} \text{ cm}^2 \text{ s}^{-1}$, which is 10 times the molecular diffusion rate, the mixing length scale, $(tK)^{1/2}$, corresponding to 1 year is *c.* 80 cm. This value is consistent with the maintenance of vertical inhomogeneity in the lake gas concentrations over distances of metres.

One possible scenario is as follows (Fig. 9). As winter progresses, gases are exsolved from the forming ice back into the residual liquid forming a bubble-free layer of ice overlying gas-charged water. Eventually, bubbles form and the water in contact with these bubbles loses gas to the bubbles. However,

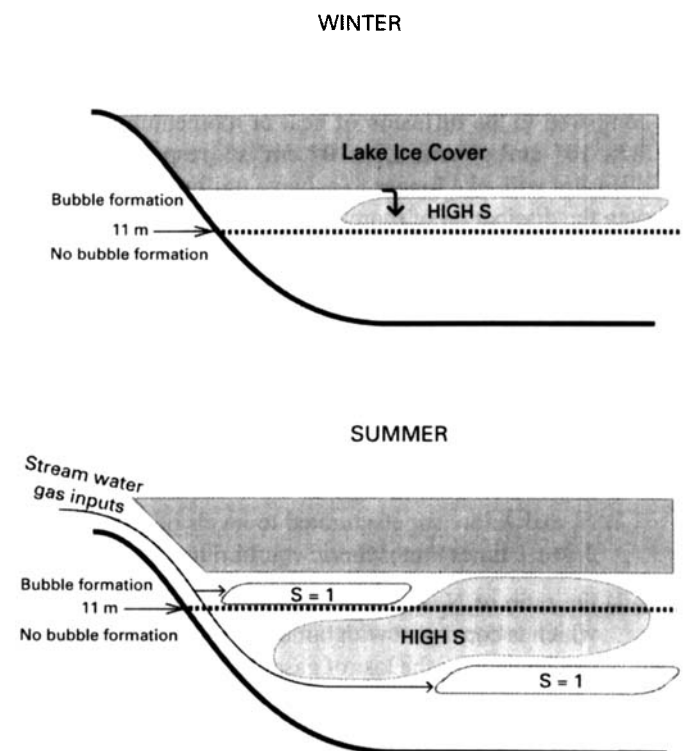


Fig. 9. Diagram of proposed model for gas supersaturation in Lake Hoare. In the winter freezing occurs at the ice water interface resulting in residual water enriched in gases and fractionated in N_2 , O_2 , and Ar concentrations (Craig *et al.* 1992). In the summer this gas enriched water is displaced by the momentum of the incoming meltwater without effectively mixing with that water. Thus parcels of water with low gas concentrations are vertically and laterally close to parcels of water with higher concentrations. Eventually diffusion will smooth out these difference but diffusion is slow without wind driven turbulence.

due to relatively low diffusion rates there is a gradient in gas concentration surrounding the bubble. Thus, at the end of winter the water column in the bubble-formation zone has a non-uniform gas concentration. When summer meltstreams flow into the lake, parcels of water are disturbed but are poorly mixed. For expected flow rates, the Reynolds number of the meltstream input is too low to induce turbulent mixing. If we consider water in the lake to flow on a flat surface (the ice cover) it will become turbulent for Reynolds numbers over 300 000 (Sissom & Pitts 1972). If instead we assume a characteristic length of 500 m (which is *c.* ½ the distance across the widest section of the lake), the velocity for the onset of turbulence is 0.1 cm s⁻¹. Alternatively, because the lake is more shallow than it is wide, we may consider the flow as in a pipe with the diameter given by the mean depth of the lake, 14.2 m. Based on this dimension the flow will become turbulent for Reynolds numbers ≥ 2000 (Sissom & Pitts 1972) implying a velocity of 0.03 cm s⁻¹. The velocity of the meltwater entering the lake is expected to be < 0.03 cm s⁻¹ and the flow is not expected to be turbulent. Precise measurements would be required to determine the velocity of water parcels in the lake. If there is non-turbulent flow, then water parcels should move in the lake without uniform mixing. Since the molecular diffusion of gas in the lake (2 × 10⁻⁵ cm² s⁻¹) is slow compared to the diffusion of heat or momentum – rates of 1.3 × 10⁻³ cm² s⁻¹ and 1.8 × 10⁻² cm² s⁻¹, respectively – gas diffusion will take longer to achieve uniform concentration than the dissipation of momentum or thermal equilibrium.

Conclusions

Measurements of dissolved gases in the water column of Lake Hoare and other Antarctic Dry Valley lakes, indicated supersaturation of the air gases. From the analysis of these measurements the following conclusions may be drawn for Lake Hoare:

- 1) N₂ and Ar are supersaturated to levels of 2.0 ± 0.37 and 3.8 ± 1.1 times atmospheric equilibrium, respectively.
- 2) the ratio of N₂ to Ar in the water column is 20.3 ± 3.8 which is consistent with bubble formation as a primary mechanism for the loss of gases from the water column.
- 3) the concentrations of N₂ and Ar are not entirely consistent with bubble formation occurring only at the ice-water interface during the freezing process. These concentrations could be explained by bubble formation to depths of *c.* 11 m.
- 4) the gas concentration in the water column is highly variable with depth but without systematic trends. This variation results when water that has been in contact with the ice moves through the lake without effective mixing.
- 5) methane has been measured in the anaerobic zone indicating the presence of methane-producing bacteria.

The absence of methane 2 m above the anaerobic region and the visual observation of what appears to be a bacterial haze at this same depth (*c.* 28 m) suggests the presence of methane-oxidizing bacteria.

- 6) there is a net flux of CO₂ upward in the water column that is approximately in balance with the measured downward flux of O₂ and, presumably, sedimentation of organic material. Within the context of an overall carbon budget, this flux balance can provide an approximation of the lake productivity.

Acknowledgements

We thank D. Mikesell, G. Noton and W. Schmidt of Antarctic Support Associates for the analysis of samples and assistance in the Antarctic, and J. Hallett, R. Landheim, D. DesMarais, C. Omelon, and B. Lyons for helpful discussions. We also thank G. Matsumoto, M. Downes, and J. Gibson for their comments and suggestions which substantially improved the manuscript. This research was supported by NASA Exobiology program and by grants to R. Wharton from NASA (NAGW-1947 and NCA2-799) and NSF (OPP-9211773).

References

- ALLNUT, F.C.T., PARKER, B.C., SEABURG, K.G. & SIMMONS JR, G.M. 1981. *In situ* nitrogen (C₂H₂)-fixation in lakes of southern Victoria Land, Antarctica. *Hydrobiological Bulletin*, **15**, 99-109.
- BACHELOR, G.K. 1967. *An introduction to fluid dynamics*. Cambridge: Cambridge University Press, 615 pp.
- BARI, S.A. & HALLETT, J. 1974. Nucleation and growth of bubbles at an ice-water interface. *Journal of Glaciology*, **13**, 489-523.
- BENSON, B.B. & KRAUSE, J.D. 1976. Empirical laws for dilute aqueous solutions of nonpolar gases. *Journal of Chemical Physics*, **64**, 689-709.
- BEVINGTON, P.R. 1969. *Data reduction and error analysis for the physical sciences*. New York: McGraw-Hill, 336 pp.
- CARTE, A.E. 1961. Air bubbles in ice. *Proceedings of the Physical Society (London)*, **77**, 757-768.
- CHINN, T.J. 1993. Physical hydrology of the Dry Valley lakes. *Antarctic Research Series*, **59**, 1-51.
- COLE, J., CARACO, N.F., KLING, G.W. & KRATZ, T.K. 1994. Carbon dioxide supersaturation in the surface waters of lakes. *Science*, **265**, 1568-1570.
- CRAIG, H. & HAYWARD, T. 1987. Oxygen supersaturation in the ocean: biological versus physical contributions. *Science*, **235**, 199-202.
- CRAIG, H., WHARTON JR., R.A. & MCKAY, C.P. 1992. Oxygen supersaturation in ice-covered Antarctic lakes: biological versus physical contributions. *Science*, **255**, 318-321.
- ELLIS, C.R., STEFAN, H.G. & GU, R. 1991. Water temperature dynamics and heat transfer beneath the ice cover of a lake. *Limnology and Oceanography*, **36**, 324-335.
- FRANZMANN, P.D., ROBERTS, N.J., MANCUSCO, C.A., BURTON, H.R. & MCMEEKIN, T.A. 1991. Methane production in meromictic Ace Lake, Antarctica. *Hydrobiologia*, **210**, 191-201.
- GALCHENKO, V.F. 1994. Sulfate reduction, methane production, and methane oxidation in various water bodies of Bunger Hills Oasis of Antarctica. *Mikrobiologia*, **63**, 683-698.

- GU, R. & STEFAN, H.G. 1990. Year-round temperature simulation of cold climate lakes. *Cold Regions Science and Technology*, **18**, 147-160.
- HENDERSON-SELLERS, B. 1985. New formulation of eddy diffusion thermocline models. *Applied Mathematical Modelling*, **9**, 441-446.
- LIPP, G., KORBER, C.H., ENGLISH, S., HARTMANN, U. & RAU, G. 1987. Investigation of the behaviour of dissolved gases during freezing. *Cryobiology*, **24**, 489-503.
- PARKER, B.C., SIMMONS JR, G.M., SEABURG, K.G., WHARTON JR, R.A. & LOVE, F.G. 1981. Modern stromatolites in Antarctic Dry Valley lakes. *BioScience*, **31**, 656-651.
- REVSBECH, N.P., MADSEN, B. & JØRGANSEN, B.B. 1986. Oxygen production and consumption in sediments determined at high spatial resolution by computer simulation of oxygen microelectrode data. *Limnology and Oceanography*, **31**, 293-304.
- SIMMONS JR, G.M., VESTAL, J.R. & WHARTON JR, R.A. 1993. Environmental regulators of microbial activity in continental Antarctic lakes. In FRIEDMANN, E.I., ed. *Antarctic microbiology*. New York: Wiley-Liss, 491-541.
- SISSOM, L.E. & PITTS, D.R. 1972. *Elements of transport phenomena*. New York: McGraw Hill, 814 pp.
- VINCENT, W.F., DOWNES, M.T. & VINCENT, C.L. 1981. Nitrous oxide cycling in Lake Vanda, Antarctica. *Nature*, **292**, 618-620.
- VINCENT, W.F. 1988. *Microbial ecosystems of Antarctica*. Cambridge: Cambridge University Press, 117-118.
- VOYTEK, M.A., PRISCU, J.C. & WARD, B.B. 1995. Detection of ammonium-oxidizing bacteria in Antarctic lake samples using the polymerase chain reaction. ASLO 1995 (abstract), University of Nevada, Reno.
- WEISS, R.F. 1970. The solubility of nitrogen, oxygen and argon in water and sea water. *Deep-Sea Research*, **17**, 721-735.
- WHARTON JR, R.W., MCKAY, C.P., CLOW, G.D. & ANDERSEN, D.T. 1993. Perennial ice-covers and their influence on Antarctic lake ecosystems. *Antarctic Research Series*, **59**, 53-70.
- WHARTON JR, R.A., MCKAY, C.P., MANCINELLI R.L. & SIMMONS JR, G.M. 1987. Perennial N₂ supersaturation in an Antarctic lake. *Nature*, **325**, 343-345.
- WHARTON JR, R.A., MCKAY, C.P., SIMMONS JR, G.M. & PARKER, B.C. 1986. Oxygen budget of a perennially ice-covered Antarctic dry valley lake. *Limnology and Oceanography*, **31**, 437-443.